

Host-Integration of a Tissue-Engineered Airway Patch: Two-Year Follow-Up in a Single Patient

Maria Steinke, PhD,^{1,2} Iris Dally, PhD,³ Godehard Friedel, MD,⁴
Heike Walles, PhD,^{1,2} and Thorsten Walles, MD FETCS⁵

Different bioengineering techniques have been applied repeatedly for the reconstruction of extensive airway defects in the last few years. While short-term surgical success is evident, there is a lack of long-term results in patients. Here, we report the case of a young male who received a 5×2 cm bioartificial airway patch for tracheoesophageal reconstruction focusing on clinical defect healing and histomorphological tissue reorganization 2.5 years after surgery. We generated bioartificial airway tissue using a cell-free biological vascularized scaffold that was re-endothelialized and reseeded with the recipient's autologous primary cells and we implanted it into the recipient's left main bronchus. To investigate host-integration 2.5 years after the implantation, we obtained biopsies of the implant and adjacent tracheal tissue and processed these for histological and immunohistochemical analyses. The early postoperative course was uneventful and the transplanted airway tissue was integrated into the host. 2.5 years after transplantation, a bronchoscopy confirmed the scar-free reconstruction of the former airway defect. Histological work-up documented respiratory airway mucosa lining the bronchial reconstruction, making it indistinguishable from native airway mucosa. After transplantation, our bioartificial airway tissue provided perfect airway healing, with no histological evidence of tissue dedifferentiation.

Introduction

NEW CONCEPTS that apply cell therapy and tissue engineering approaches have been pursued to complement surgical reconstruction maneuvers and to overcome identified shortcomings in transplantation medicine in the last decade.¹ These advanced therapies are characterized by new modes of action since viable cells belonging to the transplant integrate into the host, giving them the entire armamentarium for local and systemic biological effects. For the clinical implementation of these new therapies in patients, the above-mentioned interactions have to be monitored and understood.² To date, only few advanced therapies have been translated into the clinical setting. Therefore, knowledge regarding host-graft interaction is very limited.

Airway transplants represent a niche application in the tissue engineering field.³ However, due to the high medical need for a very small number of highly selected patients, several groups have applied tracheal airway transplants so far.^{3,4} Very recently, a thorough 5-year follow-up was published for the first patient, who received a tubular airway transplant in 2008.^{5,6}

This study confirmed the nonimmunogenic nature of autologous tissue engineering transplants in the host. However, questions remain regarding the local integration of the tissue-engineered transplant. In this study, we report the histological analysis of a tissue-engineered airway transplant that was implanted in a 26-year-old patient with an extensive post-traumatic tracheal and esophageal defect, which was biopsied 2.5 years after surgery.

Materials and Methods

Patient history

A 26-year-old male suffering from reactive depression swallowed oven cleaning detergent to commit suicide. There were no other comorbidities. The patient survived the poisoning of his upper gastrointestinal tract, including the mouth, pharynx, larynx, esophagus, and stomach, but developed an extensive long tracheoesophageal defect, extending from the distal trachea into the left main bronchus (Fig. 1A). The implantation of a tracheobronchial Y-Stent (Leufen Medical, Aachen, Germany) was not sufficient to

¹Fraunhofer Project Group Regenerative Technologies in Oncology, Würzburg, Germany.

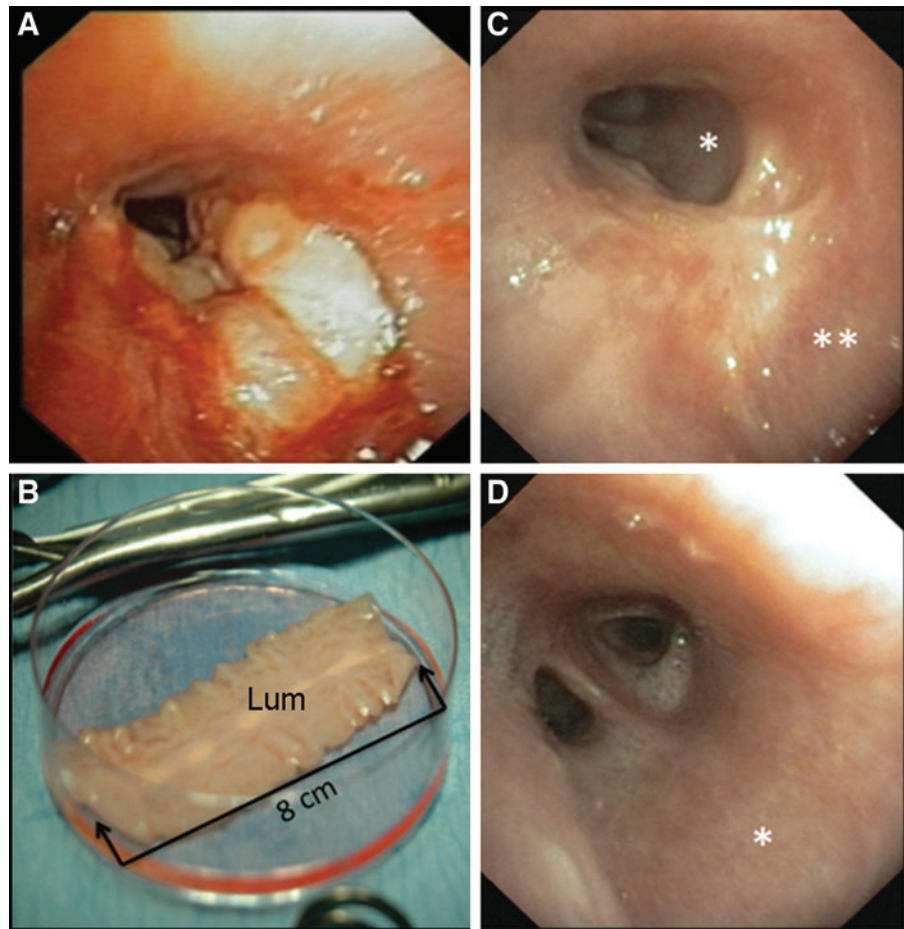
²Tissue Engineering and Regenerative Medicine, University Hospital Würzburg, Würzburg, Germany.

³Institute of Interfacial Process Engineering and Plasma Technology, University of Stuttgart, Stuttgart, Germany.

⁴Department of Thoracic Surgery, Schillerhöhe Hospital, Gerlingen, Germany.

⁵Department of Cardiothoracic Surgery, University Hospital Würzburg, Würzburg, Germany.

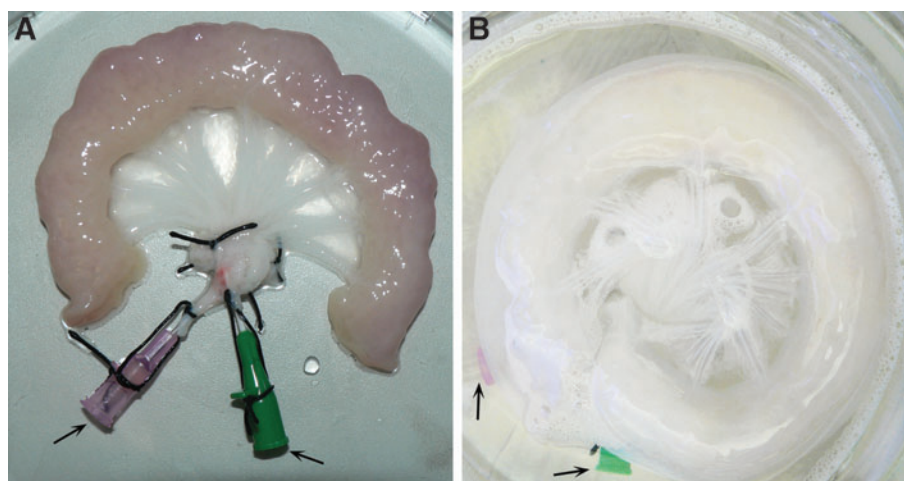
FIG. 1. Clinical implementation of the bioartificial airway patch. (A) Preoperative clinical situation with an extensive tracheoesophageal defect extending from the carina into the left main bronchus (bronchoscopy). (B) Bioartificial airway patch before trimming for surgical implantation. (C) Defect healing of the proximal and (D) distal left main bronchus following patch implantation (bronchoscopy). Sites of tissue biopsy: *, transplant; **, native airway tissue; Lum, luminal surface of the graft.



close the large tracheoesophageal and bronchoesophageal fistula and the patient suffered from recurrent bilateral pneumonia. Due to his gastric chemical burn, he was fed with the help of a jejunal feeding tube. Owing to his complex tracheoesophageal injury, the ongoing severe intrathoracic inflammatory reaction, the very limited treatment options, and the reproducible good results in previous tissue-engineered airway transplants, it was decided to offer the transplantation of an autologous bioartificial repair tissue for

airway reconstruction.^{7,8} Following patient education and informed consent, a 4 cm³ muscle biopsy was obtained from the left thigh, including a skin biopsy. The tissues were transferred into 4°C Dulbecco's modified Eagle's medium (DMEM)/Ham's F12 supplemented with 15% fetal calf serum (FCS) and endothelial cell growth medium (ECGM; Promocell, Heidelberg, Germany), respectively, and immediately transferred into the Fraunhofer Tissue Culture GMP Facilities (Fraunhofer IGB, Stuttgart, Germany). The tissue

FIG. 2. Process of airway patch generation. The biological vascularized scaffold was derived from a porcine jejunal segment (A), which was decellularized (B) by a perfusion process in a bioreactor system preserving its vascular structures and arterial (red) and venous pedicle (green) as indicated by arrows.



generation process took 6 weeks. For bioartificial tissue transplantation and airway reconstruction, the patient was positioned in a right-lateral decubitus position and a posterolateral thoracotomy was performed in the left fourth intercostal space. The tracheobronchial airway stent had been removed the day before surgery. For defect reconstruction, the left lung was deflated and the mediastinal structures were dissected, including a mobilization of the aortic arch. The cervical esophagus was diverted at the neck. The tracheoesophageal fistula was then opened and the esophageal defect was closed with an interrupted resorbable suture (Vicryl 4.0; Ethicon, Norderstedt, Germany). The effective defect extension determined intraoperatively was 5×2 cm and the generated bioartificial repair tissue was trimmed to match the defect size and sutured into the airway defect using resorbable interrupted sutures (PDS 4-0; Ethicon). For implantation, the luminal surface of the patch graft was oriented toward the tracheobronchial lumen (Fig. 1B). No tissue transpositions were performed to support secondary graft vascularization or defect closure. Intraoperative water testing confirmed air tightness. The chest was closed following standard insertion of two 28F chest drains. The tracheal cannula was removed and the tracheotomy closed surgically. Afterward the patient was transferred to the intensive care unit (ICU) for weaning from the ventilator.

On the second postoperative day, he was transferred to the normal ward. The postoperative recovery was uneventful and a bronchoscopy 8 days after surgery showed an airtight nonirritated occlusion of the airway defect. The patient was discharged from the hospital on the ninth postoperative day, was mobile, and able to speak with a powerful voice. Elective bronchoscopy 2 weeks after surgery showed initial scar tissue formation in the transplant area. The extensive esophageal defect was addressed by secondary esophageal resection and extra-anatomic reconstruction applying a retrosternal colon transplant 6 months later. To analyze the integration of the generated bioartificial repair tissue into the host's airway, we performed a flexible bronchoscopy (Fig. 1C, D) and tissue biopsy 2.5 years after surgery. By that time, the patient reported that he could eat and drink normally and was also able to play soccer.

Generation of the cell-free biological vascularized scaffold (BioVaSc[®])

For tissue generation, the autologous cells were cultured on a cell-free biological vascularized scaffold (BioVaSc[®]), as described previously^{8,9}: Porcine jejunal segments (about 12 cm long), including their mesenteric vascular supply (Fig. 2A), were resected from 12 to 15 kg piglets. Animal surgical intervention was in compliance with the Guide for Care and Use of Laboratory Animals and approved by the local animal protection board. Following explantation, 0.9% saline solution was infused through the arterial pedicle and venous return was checked. This jejunal tissue was washed to remove all remnants, followed by an overnight storage in 0.9% NaCl with 1% gentamicin, streptomycin, and penicillin at 4°C. The next day, the BioVaSc[®] was transferred into a computer-controlled closed bioreactor setup and its arterial pedicle was perfused with 500 mL of 3.4% sodium deoxycholate monohydrate for cell lysis. The perfusion pressure was regulated to 80 mmHg to avoid vessel damage.

Following removal of all chemical detergents and multiple washing steps, the cell-free scaffold (Fig. 2B) was incubated four times in 250 mL 0.9% NaCl solution for 2.5 h. Gamma-irradiation with 25 kGy (BBF Sterilisationservice GmbH, Rommelshausen, Germany) in 150 mL 0.9% NaCl solution was performed for sterilization. A small BioVaSc[®] segment was taken for quality control.

Cell isolation and cultivation

The recipient's autologous microvascular endothelial cells (mvEC) and skeletal muscle cells (SkMC) were isolated from the surgical specimen mentioned above. mvEC and SkMC were grown under standard conditions (37°C, 5% CO₂) for 4 weeks in the ECGM and in DMEM/Ham's F12 supplemented with 15% FCS, respectively, and 18×10⁶ mvEC and 12×10⁶ SkMC were achieved. The cell culture media were exchanged every 2–3 days.

Autologous re-endothelialization and reseeding of the BioVaSc[®]

For reseeding, the BioVaSc[®] was equilibrated in 30 mL ECGM at 37°C for 1 h. Then, 9×10⁶ mvEC were diluted in 2 mL ECGM and applied through the arterial pedicle for revascularization. For 24 h the cells were incubated under static conditions. Then, a second reseeding circle was performed using those cells that had adhered to the cell culture plate. After 5 days, the feeding arteries and draining veins were removed and the tubular BioVaSc[®] was opened longitudinally. For extravascular BioVaSc[®] seeding, 6×10⁶ SkMC were diluted in 1 mL DMEM/Ham's F12 supplemented with 15% FCS, transferred onto the luminal surface, and 10 mL ECGM was added. The ECGM was replaced after 24 and 72 h. After 5 days, a small segment of the bioartificial tissue was biopsied for quality control.

Histology and immunohistochemistry

The BioVaSc[®] was characterized at the end of the decellularization procedure; additionally, the airway patch was characterized, both at the time of transplantation (day 0) and 2.5 years after surgery. For histomorphological evaluation, tissue biopsies were immersion-fixed in formalin, embedded in paraffin, sectioned at 2 μm thickness, placed onto glass slides, and dried. Afterward, the samples were deparaffinized in xylene and rehydrated in a graded series of ethanol. To analyze the sample's morphology, hematoxylin and eosin (H&E) and Movat's Pentachrome staining were both performed according to standard protocols. For immunohistochemical staining, samples were rinsed in distilled water. Antigen retrieval was performed in a steamer at pH 6 to detect myosin and von Willebrand Factor (vWF) and at pH 9 to detect Cytokeratin 5 (CK 5), Cytokeratin 18 (CK 18), and beta-Tubulin. After an additional washing step, endogenous peroxidases were deactivated using 3% H₂O₂. Sections were washed and subsequently incubated for 1 h at room temperature with one of the following primary antibodies diluted in an antibody incubation buffer (catalogue #ALI20R500; DCS Innovative Diagnostik-Systeme, Hamburg, Germany): monoclonal mouse Anti-beta-Tubulin (1:2000, catalogue #T4026; Sigma-Aldrich, Schnelldorf, Germany), monoclonal mouse Anti-Human-CK 5/6 (1:200, catalogue #M7237; Dako Cytomation, Hamburg, Germany),

monoclonal mouse Anti-Human-CK 18 (1:100, catalogue #M7010; Dako Cytomation), monoclonal mouse Anti-Myosin (1:1500, catalogue #DM207-05; Acris Antibodies, Herford, Germany), and monoclonal mouse Anti-Human-vWF (1:2000, catalogue #M0616; Dako Cytomation). Excess primary antibodies were removed by washing. Detection of bound primary antibodies and chromogenic visualization with 3'3'-Diaminobenzidine were carried out using the DCS Super Vision 2 HRP-Polymer-Kit (catalogue#PD000KIT; DCS Innovative Diagnostik-Systeme), as stated by the manufacturer's instructions. After washing, the sections were counterstained with Maier's hematoxylin and blued in tap water. Samples were then dehydrated in ethanol, cleared with xylene, and coverslipped. To assure specificity of the primary antibodies, appropriate isotype antibodies were used and negative controls (omission of primary antibodies) were performed for each experiment.

MTT assay

An MTT test (Serva, Tübingen, Germany) was applied according to the manufacturer's instructions to analyze the re-endothelialization and reseeding of the airway patch concerning cell vitality. A small segment of airway patch tissue, which was not needed for surgery, was incubated for 2 h in 1 mg/mL MTT in the ECGM. The yellow MTT reagent was reduced into blue formazan by living cells and, therefore, appeared dark blue.

Light microscopic analysis

Tissue samples were evaluated with an Axio Lab.A1 (Carl Zeiss, Jena, Germany) and photographs were taken using the BZ-9000 BIOREVO System (Keyence, Neu-Isenburg, Germany). Pictures were assembled and adjusted for brightness and contrast in Adobe Photoshop CS5.

Results

Implant morphology

The BioVaSc[®] represents the cell-free structural backbone of the generated bioengineered airway patch. H&E staining reveals extracellular matrix composition consisting of villi, mucosa, and submucosa structures of the former jejunum (Fig. 3A), including preserved vascular structures (Fig. 3B) without any cellular remains. The former vascular structures of the transplant were reseeded with autologous mvEC, whereas SkMC were seeded on the transplant surface. Quality control using the MTT assay revealed successful re-endothelialization (Fig. 3C) and reseeding of the scaffold (Fig. 3D) indicated by dark blue areas.

The cells that were identified on the scaffold's surface at the time of implantation (day 0) were irregularly distributed on the graft. They could be visualized by Movat's Pentachrome staining (Fig. 4A), however, were not positive for CK 5, CK 18, and beta-Tubulin (Fig. 4B–D) in immunohistochemical stainings. Autologous SkMC and mvEC, respectively, were partly positive in myosin and vWF stainings (Fig. 4E, F).

Integrated airway transplant

2.5 years after tissue transplantation, flexible bronchoscopy found the airway transplant to be macroscopically almost

indistinguishable from the surrounding tracheobronchial tissue (Fig. 1C, D). This clinical finding was confirmed by an immunohistological work-up of the transplant biopsy, which showed the typical pseudostratified morphology of the respiratory epithelium in the Movat's Pentachrome staining, including blue-stained mucus-producing cells (Fig. 5A) with a high correlation to native tissue (Fig. 6A). In both, the transplanted airway patch and the native airway epithelium, CK 5-immunoreactive (ir) cells were detectable exclusively on the basal side of the respiratory epithelial layer (Figs. 5B and 6B), whereas CK 18-ir cells were located in the apical and basolateral region (Figs. 5C and 6C). Kinocilia were verified by beta-Tubulin immunohistochemistry in the transplanted airway patch and the adjacent native tissue (Figs. 5D and 6D). Myosin-positive cells were neither found in the connective tissue of the airway patch nor in the native lamina propria (Figs. 5E and 6E), whereas vWF-positive cells indicating the presence of endothelial cells were detected in both samples (Figs. 5F and 6F).

Discussion

In this study, we report about the successful reconstruction of an extensive tracheoesophageal defect with the help of a tissue-engineered airway transplant and the histomorphological characterization of the transplanted tissue. Biopsy analysis 2.5 years after surgery verified long-term patch integrity and tissue reorganization: the luminal surface of the airway patch was covered with an autologous pseudostratified respiratory epithelium, which was indistinguishable from native airway epithelium. The morphologically intact respiratory epithelium consisted of undifferentiated CK 5-ir and differentiated CK 18-ir epithelial cells, indicating epithelial regeneration and differentiation processes. Mucus-producing goblet cells and kinocilia located on the apical side of the airway epithelium suggest a functional mucociliary clearance. The absence of probably degraded myosin-ir cells and the presence of vWF-ir endothelial cells 2.5 years after transplantation also confirm tissue reorganization and long-term patch integrity.

The generated tissue transplant provided the means for the reconstruction of an extensive tracheoesophageal colliquative necrosis, for which normally no established surgical treatment options are available. We hypothesize that the capillary network of our transplant established the foundation for untroubled tissue ingrowth and airway healing since there was no relevant endobronchial scar tissue formation or airway malacia. Initial scar tissue formation that was observed 2 weeks after surgery had regressed. These results confirm our previous report in another patient 6 months after airway reconstruction that the tissue-engineered transplant facilitates the complete regeneration of the airway defect.¹⁰ The transplanted tissue undergoes a pronounced remodeling process after implantation and we assume that it is completely replaced by host tissue.

For treatment of end-stage organ failure in the aging population, the demand for organs is escalating, whereas the supply has reached a plateau.¹¹ At the same time, some complex organ and tissue injuries still have few therapeutic options.¹ Recent advances in the field of tissue engineering and regenerative medicine have provided proof of principle that these technologies may be applicable to overcome the

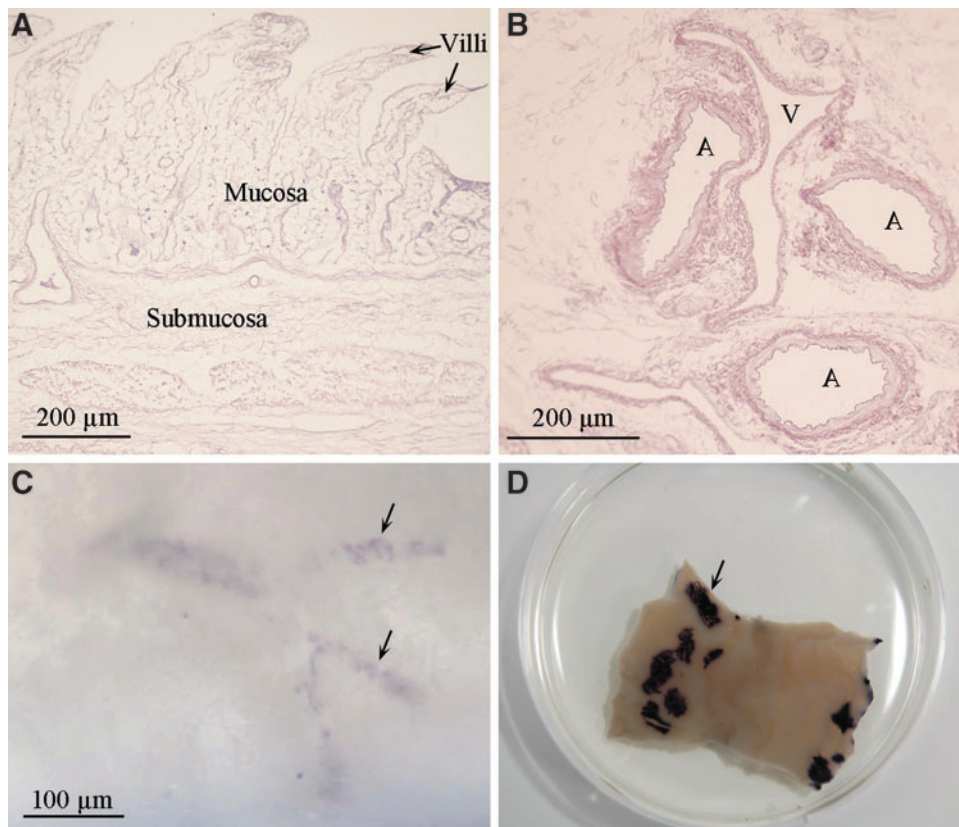


FIG. 3. Quality control during airway patch generation. Hematoxylin and eosin staining of the apical (A) and basal region (B) of the decellularized scaffold reveals the extracellular matrix of the former jejunum without cellular residues. The MTT assay shows successful re-endothelialization with microvascular endothelial cells (C) and reseeding with skeletal muscle cells (D). Arrows in (C, D) exemplarily point to MTT-positive areas. A, artery; V, vein.

identified shortcomings. Since these advanced therapies are characterized by new modes of action, a fundamental understanding of their long-term effects is mandatory. Substitutes for the human trachea and its bronchial tree represent a niche application in this rapidly growing sci-

entific field. However, several different airway bioengineering approaches have already been translated into the clinical setting and applied in patients.^{3,4} Short-term follow-up in these applications identified the critical role of respiratory epithelium lining the transplant for graft function.

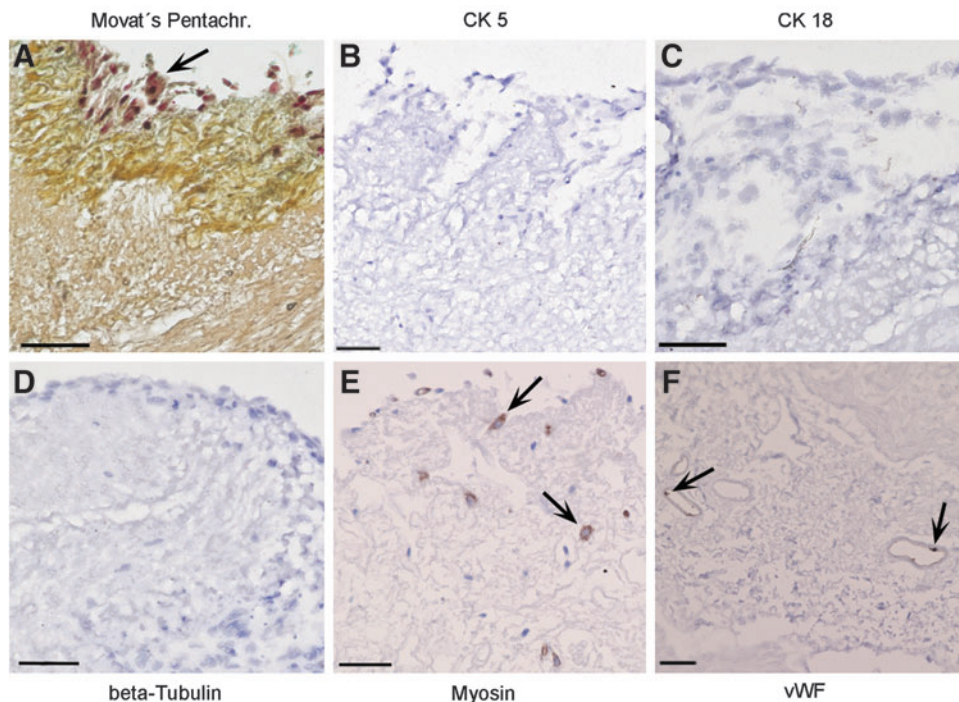
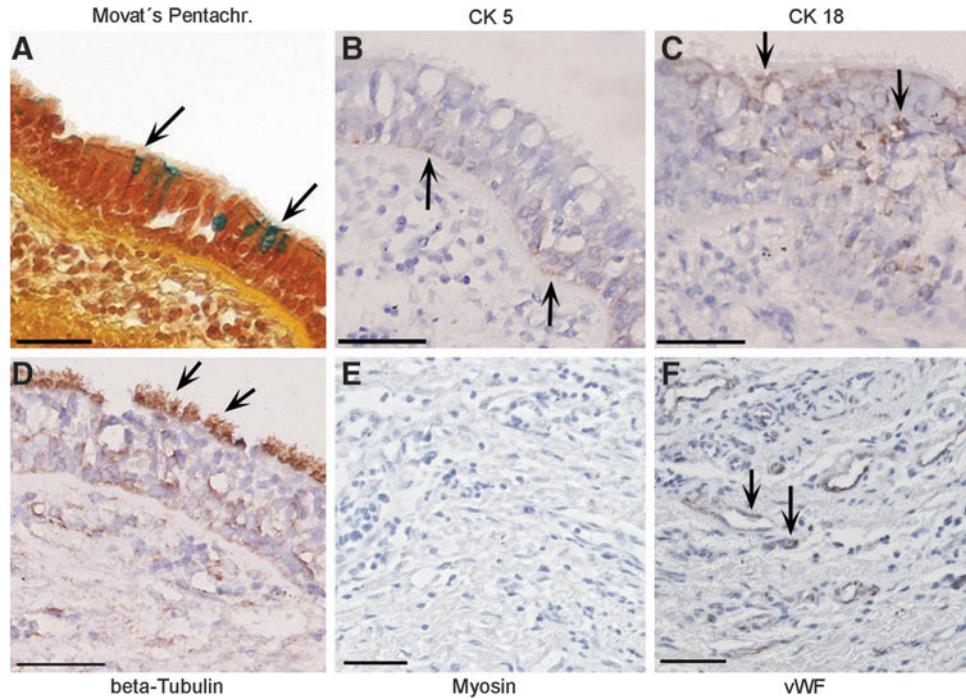


FIG. 4. Histological and immunohistochemical characterization of the airway patch at day 0. At time of implantation, in the tissue transplant, only irregularly distributed cells were observed in Movat's Pentachrome staining (A), which were not stained for Cytokeratin 5 (CK 5) (B), Cytokeratin 18 (CK 18) (C), and beta-Tubulin (D), however, showed positive immunostaining for myosin (E) and von Willebrand Factor (vWF) (F) as exemplarily indicated by arrows. All scale bars: 50 μm.

FIG. 5. Histological and immunohistochemical characterization of the airway patch 2.5 years after transplantation. The surface of the airway patch has changed into respiratory epithelium, including mucus-producing cells (arrows in A), CK 5-, CK 18-, and beta-Tubulin-positive cells (arrows in B–D, respectively). Whereas myosin-immunoreactive cells were not detected (E), vWF-positive cells were visible in vascular structures (arrows in F). All scale bars: 50 μ m.

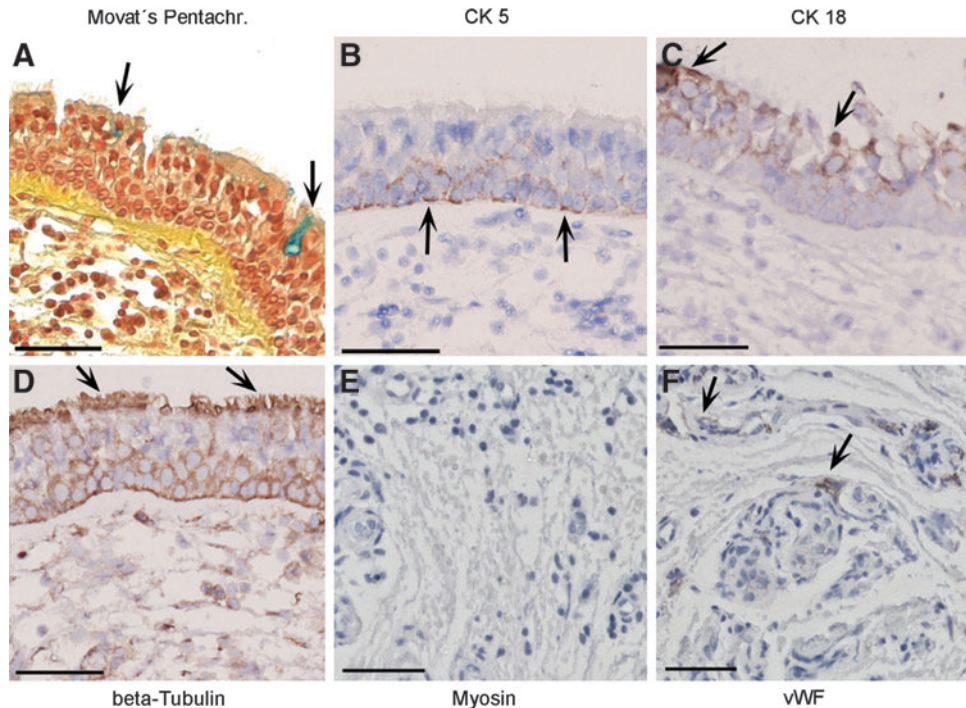


The generation of our airway patch lasted 6 weeks, which is definitely a disadvantage of this above-presented approach. Recently, Macchiarini *et al.* reported the successful generation and transplantation of a tubular airway transplant in a patient with severe malacia.⁶ The scaffold of their tissue transplant was a cadaver trachea, which was decellularized and reseeded with autologous cells of the recipient. The generation of their transplant lasted 6 weeks as well. In a recent 5-year follow-up, they published a thorough clinical and histological work-up of their patient.⁵ They reported a

progressive cicatricial stenosis at the proximal graft anastomosis, adequate secondary transplant vascularization, and a complete respiratory epithelial lining of the graft with normal ciliary function.

Our 2.5-year follow-up study underlines the high suitability of tissue-engineered airway tissues for tracheobronchial repair. Despite the different nature of airway reconstruction realized by Macchiarini *et al.*,⁶ which implies circumferential removal of a segment of bronchi, while our reconstruction was only the membranous part of the trachea, we did not encounter any

FIG. 6. Histological and immunohistochemical characterization of patient's native trachea biopsy. Movat's Pentachrome staining shows pseudostratified airway epithelium with mucus-producing cells (arrows in A). Arrows in (B–D, and F) exemplarily indicate CK 5-, CK 18-, beta-Tubulin-, and vWF-immunoreactive areas. No myosin-positive cells were found (E). All scale bars: 50 μ m.



relevant scar formation. We believe that our pre-existing autologous vascular network inside our airway transplant supports its integration into the host's vascular system by sending out paracrine signals to induce secondary vascularization for both the transplant environment and transplant vascularization, which is supported by previous *in vitro* data.¹² We are convinced that any transplanted bioartificial tissue—as any normal tissue—depends on sufficient vascularization to survive and maintain its physiology. Thus, our tissue-engineered airway patch affords perfect airway healing following transplantation with no histological evidence of tissue dedifferentiation.

Acknowledgments

This work was financially supported by the German Research Foundation (WA 1649/3-1) and the Federal Ministry of Education and Research (FKZ 0315575). The authors are indebted to Christa Amrehn (University Hospital Würzburg, Tissue Engineering and Regenerative Medicine, Germany), Sylvia Kolbus-Hernandez, and Brigitte Höhl (Fraunhofer Institute for Interfacial Engineering and Biotechnology IGB, Stuttgart, Germany) for excellent technical assistance, to Markus Schandar for supervising the patch generation process and to Victoria Andreas for critical revision.

Disclosure Statement

T.W. has two issued patents EP1500697 and DE10333863 related to the BioVaSc[®] generation. No competing financial interests exist for the other authors.

References

1. Badylak, S.F., Weiss, D.J., Caplan, A., and Macchiarini, P. Engineered whole organs and complex tissues. *Lancet* **379**, 943, 2012.
2. Guthrie, K., Bruce, A., Sangha, N., Rivera, E., and Basu, J. Potency evaluation of tissue engineered and regenerative medicine products. *Trends Biotechnol* **31**, 505, 2013.
3. Walles, T. Tracheobronchial bio-engineering: biotechnology fulfilling unmet medical needs. *Adv Drug Deliv Rev* **63**, 367, 2011.
4. Jungebluth, P., and Macchiarini, P. Airway transplantation. *Thorac Surg Clin* **24**, 97, 2014.
5. Gonfiotti, A., Jaus, M.O., Barale, D., Baiguera, S., Comin, C., Lavorini, F., Fontana, G., Sibila, O., Rombola, G., Jungebluth, P., and Macchiarini, P. The first tissue-engineered airway transplantation: 5-year follow-up results. *Lancet* **383**, 238, 2014.
6. Macchiarini, P., Jungebluth, P., Go, T., Asnaghi, M.A., Rees, L.E., Cogan, T.A., Dodson, A., Martorell, J., Bellini, S., Parnigotto, P.P., Dickinson, S.C., Hollander, A.P., Mantero, S., Conconi, M.T., and Birchall, M.A. Clinical transplantation of a tissue-engineered airway. *Lancet* **372**, 2023, 2008.
7. Macchiarini, P., Walles, T., Biancosino, C., and Mertsching, H. First human transplantation of a bioengineered airway tissue. *J Thorac Cardiovasc Surg* **128**, 638, 2004.
8. Mertsching, H., Schanz, J., Steger, V., Schandar, M., Schenk, M., Hansmann, J., Dally, I., Friedel, G., and Walles, T. Generation and transplantation of an autologous vascularized bioartificial human tissue. *Transplantation* **88**, 203, 2009.
9. Mertsching, H., Walles, T., Hofmann, M., Schanz, J., and Knapp, W.H. Engineering of a vascularized scaffold for artificial tissue and organ generation. *Biomaterials* **26**, 6610, 2005.
10. Walles, T., Biancosino, C., Zardo, P., Macchiarini, P., Gottlieb, J., and Mertsching, H. Tissue remodeling in a bioartificial fibromuscular patch following transplantation in a human. *Transplantation* **80**, 284, 2005.
11. Orlando, G., Soker, S., and Stratta, R.J. Organ bioengineering and regeneration as the new Holy Grail for organ transplantation. *Ann Surg* **258**, 221, 2013.
12. Schanz, J., Pusch, J., Hansmann, J., and Walles, H. Vascularised human tissue models: a new approach for the refinement of biomedical research. *J Biotechnol* **148**, 56, 2010.

Address correspondence to:

Maria Steinke, PhD

Fraunhofer Project Group Regenerative

Technologies in Oncology

Röntgenring 11

Würzburg 97070

Germany

E-mail: maria.steinke@uni-wuerzburg.de

Received: April 11, 2014

Accepted: September 4, 2014

Online Publication Date: December 10, 2014